




# Extraction of indene from local pyrolysis oil and its usage for synthesis of a cationite

Saidmansur Saidobbozov<sup>1</sup> · Suvonqul Nurmanov<sup>1</sup> · Orifjon Qodirov<sup>1</sup> · Askar Parmanov<sup>1</sup> · Samadjon Nuraliyev<sup>1</sup> · Elyor Berdimurodov<sup>2,3,4</sup> · Ahmad Hosseini-Bandegharai<sup>5,6,7,8</sup>  · Wan Mohd Norsani B. Wan Nik<sup>9</sup> · Asmaa Benettayeb<sup>10,11</sup> · Nabisab Mujawar Mubarak<sup>12,13</sup> · Khasan Berdimuradov<sup>14,15</sup>

Received: 4 May 2024 / Revised: 23 August 2024 / Accepted: 27 August 2024  
© The Author(s), under exclusive licence to the Institute of Chemistry, Slovak Academy of Sciences 2024

## Abstract

Keeping the principles of sustainability in view, this work explores the extraction of indene from pyrolysis oil—a complex by-product of the Ustyurt Gas-Chemical Complex—and its transformation into a novel cationite, highlighting sustainable approaches in chemical engineering and material science. Utilizing advanced analytical techniques, including thermogravimetric analysis (TG), chromato-mass spectrometry, and Fourier-transform infrared spectroscopy (FT-IR), indene was efficiently isolated and characterized. The indene extracted exhibited a principal ion peak at a molecular mass ( $m/z$ ) of 117.0, confirming its purity and potential for further applications. Following extraction, indene underwent sulfonation and polycondensation with 35% formalin under specific conditions (100–110°C, 30–40 atm), resulting in a cationite with a yield of 71%. This synthesized IESA (indene-based sulfonated aromatic cation exchanger), demonstrated significant chemical–physical properties when compared to commercial equivalents, such as a moisture content significantly lower than the KU-2-8 (29.4% vs. 48–58%), and a dynamic exchange capacity (DEC) competitive with industry standards (472 mmol/m<sup>3</sup> vs. 500–520 mmol/m<sup>3</sup>). The study not only showcases the potential of pyrolysis oil as a valuable feedstock for producing high-value chemical products, but also advances the development of new materials from industrial by-products.

**Keywords** Pyrolysis oil · Indene extraction · Cationite synthesis · Ion exchange resin · Sulfonation · Polycondensation

## Introduction

Chemical engineering and material science continuously drive advancements in sustainable development and resource optimization. A critical challenge in these disciplines is the valorization of industrial by-products to minimize waste and enhance economic viability (Miettinen et al. 2024; Zeidabadi et al. 2024; Mamchenko and Pakhar 2024). Pyrolysis oil, a by-product generated through the thermal decomposition of organic materials in an inert atmosphere, represents a complex mixture of hydrocarbons and other organic compounds with significant potential applications (Busche et al. 2024; Gong et al. 2024; Munangi et al. 2024). Despite its rich chemical profile, the practical utilization of pyrolysis oil has been hindered by its intricate composition and the difficulty in isolating valuable constituents. Among these compounds, indene stands out due to its potential applications in synthesizing

high-performance polymers, pharmaceuticals, and ion exchange resins (cationites). The extraction and purification of indene from pyrolysis oil require advanced analytical and separation techniques, such as thermogravimetric analysis (TG), chromato-mass spectrometry, and Fourier-transform infrared spectroscopy (FT-IR). These techniques not only facilitate the identification and isolation of indene, but also ensure its purity and suitability for subsequent chemical transformations. (Choi et al. 2020; Al-Asheh and Aidan 2020; Huang et al. 2021). The valorization of pyrolysis oil through the efficient extraction of indene and its conversion into functional materials addresses both environmental sustainability and economic considerations. This research aims to develop a reliable process for isolating indene from pyrolysis oil and demonstrate its utility in synthesizing a novel cationite. By leveraging indene's chemical properties, we can enhance the performance characteristics of ion exchange resins, offering a viable alternative to petrochemical-derived products and contributing to the circular economy (Vincio

Extended author information available on the last page of the article

et al. 2022; Lebron et al. 2021; Lee et al. 2020; Dixit et al. 2021).

There are various difficulties in the process of extracting and using compounds from pyrolysis oil. The main problem is with the separation procedure; in order to recover pure chemicals from the complicated pyrolysis oil, advanced separation techniques are needed. Because of these difficulties with separation, indene is frequently disregarded despite its importance (Sarchami et al. 2021; Toteva and Stanulov 2020; Sekar et al. 2022; Rasouli et al. 2024). Furthermore, petrochemical sources—which are limited and worsen environmental conditions—are a major component of the commercial manufacture of ion exchange resins. Alternative energy sources that are environmentally friendly, sustainable, and need less energy are therefore desperately needed (Sekar et al. 2021; Bakar et al. 2020; Tao et al. 2020; Dong et al. 2024).

An important first step in the process of making this by-product more valuable is the extraction of indene from pyrolysis oil. To separate and purify indene, advanced analytical techniques are used in the process (Cai et al. 2023; Li et al. 2020; Kuan et al. 2023). This study uses a driving approach in a typical laboratory setting, followed by in-depth examination with TG analysis, chromato-mass spectrometry, and FT-IR spectroscopy, among other tools. These techniques guarantee the effective extraction of indene and open the door to the analysis of its yield and purity, two essential factors for its future uses (Ramdas, et al. 2020; Liao and Zhao 2022).

Previous studies have highlighted the potential of pyrolysis oil in various applications, including its use as a feedstock for producing high-value chemicals. Choi et al. (2020) demonstrated the sequential recovery of valuable metals from bioleached wastewater using ion exchange resins derived from pyrolysis oil (Choi et al. 2020). Al-Asheh and Aidan (2020) discussed comprehensive methods for regenerating ion exchange resins for water treatment, emphasizing the importance of effective separation techniques (Al-Asheh and Aidan 2020). Huang et al. (2021) explored the removal of colorants using ion exchange resins, indicating the versatility of these materials in industrial processes. Despite these advancements, the extraction and purification of specific valuable compounds like indene from pyrolysis oil remain underexplored. The current methods often struggle with efficiency and purity, limiting the broader application of these compounds (Ku et al. 2024; Jasim and Ajjam 2024; Abusultan et al. 2024). While there is substantial research on the general applications of pyrolysis oil, there is a noticeable gap in the literature regarding the efficient extraction and utilization of indene for high-performance applications. Existing studies primarily focus on broader applications without delving into specific extraction processes and their optimization.

This research uniquely addresses the challenge of isolating indene from pyrolysis oil and transforming it into a novel cationite. By focusing on advanced analytical and separation techniques, this study aims to bridge the gap in the current literature and provide a detailed methodology for the efficient extraction of indene. The primary aim of this research is to develop a reliable process for isolating indene from pyrolysis oil and demonstrate its utility in synthesizing a novel cationite. The specific objectives are:

To establish an effective method for extracting indene from pyrolysis oil using advanced analytical techniques such as thermogravimetric analysis (TG), chromato-mass spectrometry, and Fourier-transform infrared spectroscopy (FT-IR).

To synthesize a cationite from the extracted indene through sulfonation and polycondensation processes.

To compare the chemical–physical properties of the synthesized cationite with commercial equivalents, focusing on moisture content, density, and dynamic exchange capacity (DEC).

To highlight the environmental and economic benefits of utilizing pyrolysis oil as a feedstock for producing high-value chemical products.

By achieving these objectives, this research aims to contribute significantly to the fields of material science and chemical engineering, promoting sustainable practices and efficient resource utilization.

## Materials and methods

### Materials

#### Pyrolysis oil

In this study, pyrolysis oil, obtained as a by-product from the Ustyurt Gas-Chemical Complex operated by “Uz-Kor Gas Chemical” LLC in Uzbekistan, served as the primary raw material. To isolate indene along with other constituents from pyrolysis oil, a distillation method was employed within standard laboratory settings.

#### Chemicals

The chemicals required for the experiments, including sulfuric acid ( $\text{H}_2\text{SO}_4$ ) with a density of 1.84 g/ml and purity of 98%, formaldehyde (HCHO) in the form of formalin at 35% concentration, sodium chloride (NaCl), calcium hydroxide ( $\text{Ca}(\text{OH})_2$ ), sodium carbonate ( $\text{Na}_2\text{CO}_3$ ), and other essential reagents, were supplied by Qingdao Sigma Chemical Co., Ltd., based in Qingdao, China. All solvents and substances were controlled according to specific standards and

monitored by TLC in hexanes on Merck silica gel 60F254 (Germany) plates. Analytical pure substances were used.

## Methods

For the spectroscopic analysis of chemical compounds, a Bruker Invenio S-2021 Fourier-transform infrared spectrometer, located in Tokyo, Japan, was utilized. This analysis was conducted across a wavenumber range of 4000 to 400  $\text{cm}^{-1}$ , with the OPUS software employed for the visualization of the FT-IR spectra (Prsyazhnyi et al. 2023; Pyshyev, et al. 2023; McCabe et al. 2020; Oates et al. 2023). Thermogravimetric analysis was performed using a DTG-60 Simultaneous DTA-TG Apparatus by Shimadzu, Japan. The temperature for these analyses ranged from 25 to 500 °C. The morphological and elemental analysis of samples was conducted using a SEM/EDS-Zeiss EVO MA10 system by Carl Zeiss Microscopy GmbH, Jena, Germany. Moisture content was measured with a precision moisture meter (model: XЙ-100MW, Serial Number: 201810066, Maximum capacity: 110 g, Accuracy: 0.001 g, Margin of error: 0.002 g). For the chromatography–mass spectrometry analysis, an Agilent Technologies 7890 N Network GC System equipped with a 5977 A MSD detector was used following the DRUGS\_SKAN. A1 M protocol (Pigot et al. 2022; Sun et al. 2022; Zhuang et al. 2021; Dumur 2021; Suo et al. 2022). The database used for mass spectra interpretation in this study is the (gas chromatography–mass spectrometry) GCMS base, specifically employing the following libraries: A-libN02W275.M; A-libW11N17.M; and A-libW11N14.M. These libraries were utilized to interpret the mass spectra obtained during the chromatographic and mass spectrometric analyses of the extracted indene and other compounds from pyrolysis oil.

## Study of physicochemical properties of IESA (indene-based sulfonated aromatic cation exchanger)

The experimental procedures were conducted in strict accordance with the international standard GOST 10896–78 (Uzbekistan, which is specifically designed for the testing of indene-based polyindenesulfonic acid intended for use as a cation exchange resin (cationite). This standard outlines the requisite preparation methods to accurately assess the physicochemical and technological attributes of ion exchange materials.

Step-by-Step Procedure of preparation:

1. Isolation of Indene from Pyrolysis Oil: The preparation of the indene-based sulfonated aromatic (IESA) cation exchanger from pyrolysis oil begins with the isolation of indene. Pyrolysis oil, obtained from the Ustyurt Gas-Chemical Complex, is subjected to fractional distilla-

tion, and the fraction boiling in the range of 179–189 °C, which primarily contains indene, 1-methylindene, and tetralin, is collected.

2. Characterization of Indene: The isolated indene is characterized using Fourier-transform infrared spectroscopy (FT-IR) to verify its chemical structure, thermogravimetric analysis (TGA) to assess its thermal properties, and gas chromatography–mass spectrometry (GC–MS) to determine its purity and molecular mass ( $m/z$ ).
3. Sulfonation of Indene: For the sulfonation of indene, 100 g of indene is mixed with sulfuric acid ( $\text{H}_2\text{SO}_4$ ) in a 1:1.2 molar ratio, and the reaction mixture is maintained at a temperature of 100–120 °C for 4 h. After the reaction, the mixture is cooled, and water is carefully added to dilute it.
4. Neutralization and Precipitation: The diluted sulfonated indene mixture is neutralized by adding a calcium hydroxide ( $\text{Ca}(\text{OH})_2$ ) solution, and vacuum filtration using a Buchner funnel is employed to remove insoluble materials. Sodium carbonate ( $\text{Na}_2\text{CO}_3$ ) is then added to the filtrate to precipitate the sodium salt of indene-sulfonic acid. The precipitate is collected by filtration and washed with distilled water until a neutral pH is achieved.
5. Polycondensation Reaction: The purified indenesulfonic acid undergoes a polycondensation reaction by dissolving it in formalin (35% formaldehyde solution) in a 1:1.4 molar ratio. This mixture is placed in a pressure vessel and heated at 100–110 °C under 30–40 atm pressure for 12 h. After the reaction, the vessel is cooled, and the solid cation exchanger is collected.
6. Purification and Drying: The solid product is then washed with distilled water to remove any residual reactants and dried at 100–105 °C for 12 h to obtain the final IESA cation exchanger.

The final moisture content was accurately determined using a precision moisture meter (model: XY-100 MW, Serial Number: 201810066, with a maximum capacity of 110 g, an accuracy of 0.001 g, and a margin of error of 0.002 g).

## Results and discussion

### Physical properties of selected pyrolysis oil

The analysis of the pyrolysis oil reveals it as an oily liquid characterized by an unpleasant odor and a color ranging from light brown to light green. The physical properties detailed in Table 1 provide a foundational understanding of the oil's characteristics:

Density at 200 °C is measured at 1.064 g/cm<sup>3</sup>, indicating the oil's relative heaviness compared to water. This density is crucial for separation and purification processes.

Kinematic viscosity at 1000 °C stands at 38 mm<sup>2</sup>/s, suggesting the oil's flow behavior under extreme heat, which impacts its handling and transport.

Coking percentage is recorded at 14%, highlighting the potential residue formation upon heating, affecting its utility in thermal processes.

Water content at 0.3% demonstrates low moisture level, which is advantageous for many applications requiring dry conditions.

Mechanical impurities are minimal, at 0.01%, indicating a relatively clean oil that may reduce processing challenges.

Evaporation temperature is observed at 195 °C, providing insights into the oil's volatility and the temperatures required for its distillation.

The elemental composition underscores a high carbon content (91.3%), alongside other elements such as sulfur (7.9%) and traces of sodium (Na<sup>+</sup>), potassium (K<sup>+</sup>), and other elements, informing about the oil's potential applications and environmental considerations.

### Chromato-mass analysis of pyrolysis oil

The chromato-mass spectrum of pyrolysis oil, as illustrated in Table 2 and Fig. 1, sheds light on the oil's complex chemical makeup, offering potential pathways for its valorization:

- Hydrocarbons, including benzene (0.17%), ethenylbenzene (0.29%), and a significant presence of C3-Benzene (28.92%), underline the oil's rich composition suitable for chemical feedstocks.
- The presence of 1H-Indene in notable percentages (24.67%) highlights the oil's potential as a source for specific valuable chemicals.
- Naphthalene and its derivatives, like methylnaphthalene (0.22%) and azulín (5.62%), suggest the oil's utility in producing chemicals for the dye industry and other sectors.

The variety of identified compounds, such as 1-Methyl-3-Ethylbenzene (6.16%) and 1,2,4-Trimethylbenzene (4.00%), further illustrates the pyrolysis oil's complexity and the potential for extracting diverse chemical products.

The analysis of the pyrolysis oil's physical properties and chemical composition underscores its potential as a versatile resource for various industrial applications. However, the challenges related to its processing, such as high coking percentage and the presence of impurities, require innovative solutions to fully exploit this resource. The high carbon content and specific valuable compounds like indene open

**Table 1** Physical properties of pyrolysis oil

Properties	Obtained values
Density at 200 °C (g/cm <sup>3</sup> )	1.064
Kinematic viscosity at 1000 °C (mm <sup>2</sup> /s)	38
Coking (%)	14
Water content (%)	0.3
The amount of mechanical impurities (%)	0.01
Evaporation temperature (°C)	195
Element composition, % by mass	
C	91.3
S	7.9
Na <sup>+</sup>	0.14
K <sup>+</sup>	0.01
Other elements:	0.001
	0.649

avenues for sustainable chemical production provided that effective separation and purification methods are developed.

Pyrolysis oil is a complex mixture comprising various organic and inorganic components. The organic components include hydrocarbons such as aliphatic hydrocarbons, aromatic hydrocarbons (e.g., benzene, toluene, indene), and polycyclic aromatic hydrocarbons (PAHs) like naphthalene. Additionally, it contains oxygenated compounds such as phenols, alcohols (e.g., methanol, ethanol), carboxylic acids (e.g., acetic acid), and ketones (e.g., acetone). Nitrogenous compounds such as amines and nitriles, as well as sulfur compounds like thiophenes, are also present. The inorganic components include metals like sodium (Na), potassium (K), calcium (Ca), magnesium (Mg), and iron (Fe), along with mineral ash consisting of silica, alumina, and other minerals. Furthermore, salts such as sodium chloride (NaCl) and other chloride salts are found in pyrolysis oil (Wang et al. 2024; Yan et al. 2024). These diverse components define the composition and properties of pyrolysis oil, making it a complex yet valuable source for extracting various chemicals and materials.

### Fractional composition of pyrolysis oil

The fractional distillation of pyrolysis oil yields ten distinct fractions, each with varying concentrations of hydrocarbons, demonstrating the complex nature of pyrolysis oil. Notably (Tables 3 and 4, Fig. 2):

Fraction 1 (179–189 °C) primarily contains indene, 1-methylindene, and tetralin, making up 70% of this fraction's composition, showcasing the high concentration of valuable chemicals in the initial distillation range.

Fraction 2 (210–220 °C) is predominantly naphthalene, comprising up to 96% of the fraction. This fraction

**Table 2** Chromato-mass spectrum results of pyrolysis oil

No	Name	Mass percentage, %
1	Benzene	0.17
2	Ethenylbenzene	0.29
3	Allylbenzene	0.30
4	1-Propylbenzene	0.48
5	1-Methyl-3-Ethylbenzene	6.16
6	1,2,4-Trimethylbenzene	4.00
7	1-Methyl-4-Ethylbenzene	3.25
8	C3-Benzene	28.92
9	Phenylethyl alcohol	0.50
10	1,2,3-Trimethylbenzene	4.53
11	1H-Indene	24.67
12	M-Propyltoluene	2.43
13	1,4-Dimethyl-2-Ethylbenzene	3.60
14	4-Ethyl-O-Xylene	1.77
15	1,3-Dimethyl-2-Ethylbenzene	2.60
16	1-Phenyl-2-Methylpropane	0.26
17	Bicyclohexane	0.44
18	5-Ethyl-M-Xylene	0.23
19	1-Methyl-2-Isopropylbenzene	1.93
20	O-Alkyltoluene	0.39
21	P-Methylallyl Benzene	0.75
22	1-Methylindene	2.85
23	1-Butynyl Benzene	1.47
24	Naphthalene	0.76
25	Azolin	5.62
26	Methylnaphthalene	0.22

constitutes 37% of the total distilled product, highlighting naphthalene's significant presence in pyrolysis oil.

Fraction 3 (220–235 °C) still features naphthalene, alongside its methyl derivatives, accounting for 85% of this fraction. This suggests the availability of chemically similar compounds within a narrow distillation range, potentially simplifying separation processes for these compounds.

Subsequent fractions up to Fraction 10 diversify into other compounds such as diphenyl, acenaphthene, and even fullerene, each dominating their respective fractions. This diversification underscores the rich chemical reservoir within pyrolysis oil, offering numerous avenues for chemical extraction and application.

The analysis of Fraction 1 through chromato-mass spectrometry further delineates the composition, with compounds like C3-Benzene (28.92%) and 1H-Indene (24.67% combined for two peaks) standing out. This detailed breakdown not only reaffirms the complexity of pyrolysis oil, but also highlights specific compounds of interest for further applications.

## Chromo-mass spectrum of indene isolated from pyrolysis oil

The chromato-mass spectrometric analysis of purified indene demonstrates a principal ion peak at a molecular mass ( $m/z$ ) of 117.0, indicative of the molecular weight of indene. The presence of several fragment ions with  $m/z$  values of 103, 91, 77, 51, 39, and 26 further elucidates the breakdown patterns of the indene molecule under ionization conditions. These fragment ions are indicative of the structural components of indene, shedding light on its stability and reactivity (Fig. 3):

- The ion at  $m/z = 103$  suggests a loss of a methyl group ( $\text{CH}_3$ , 14 Da) from the parent indene ion, possibly indicating the presence of substituted indene derivatives.
- $m/z = 91$  is characteristic of a benzyl cation, a common fragment observed in the mass spectra of aromatic compounds, supporting the aromatic nature of indene.
- The fragment at  $m/z = 77$  corresponds to a tropylium ion, further suggesting the stability of the seven-membered ring structure within the indene molecule upon ionization.
- Smaller fragments ( $m/z = 51, 39, 26$ ) likely result from further breakdown of the indene molecule, offering insights into the bonding and structural arrangement within the molecule.

## IR analysis of indene isolated from pyrolysis oil

The IR spectrum of indene elucidates its molecular structure by identifying specific functional groups, offering a detailed view into its chemical composition (Fig. 4). Peaks at  $3019\text{ cm}^{-1}$  and  $2983\text{ cm}^{-1}$  signify the presence of  $\text{C-H}$  stretching vibrations, typical for aromatic and alkene groups, respectively, underscoring indene's unsaturated nature. The absorption at  $2921\text{ cm}^{-1}$  suggests aliphatic  $\text{C-H}$  stretching, indicating methyl or methylene groups attached to the indene ring. A peak at  $2730\text{ cm}^{-1}$  could be tied to overtone or combination bands often seen in aromatic compounds. The band at  $1607\text{ cm}^{-1}$  indicates  $\text{C=C}$  stretching vibrations within the aromatic ring, affirming indene's aromatic structure. Absorptions at  $1456\text{ cm}^{-1}$  and  $1377\text{ cm}^{-1}$ , characteristic of  $\text{C-H}$  bending in methyl and methylene groups, support the presence of alkyl substituents on the indene ring. A sharp peak at  $751\text{ cm}^{-1}$  points to out-of-plane bending vibrations of hydrogen atoms on the aromatic ring, typical for disubstituted benzene rings, which is consistent with the structure of indene. Lastly, the peak at  $668\text{ cm}^{-1}$  likely corresponds to  $\text{C-H}$  out-of-plane bending, further confirming the aromatic nature of indene. This comprehensive molecular fingerprint provided by the IR spectrum confirms indene's structural and functional attributes through detailed spectroscopic analysis.



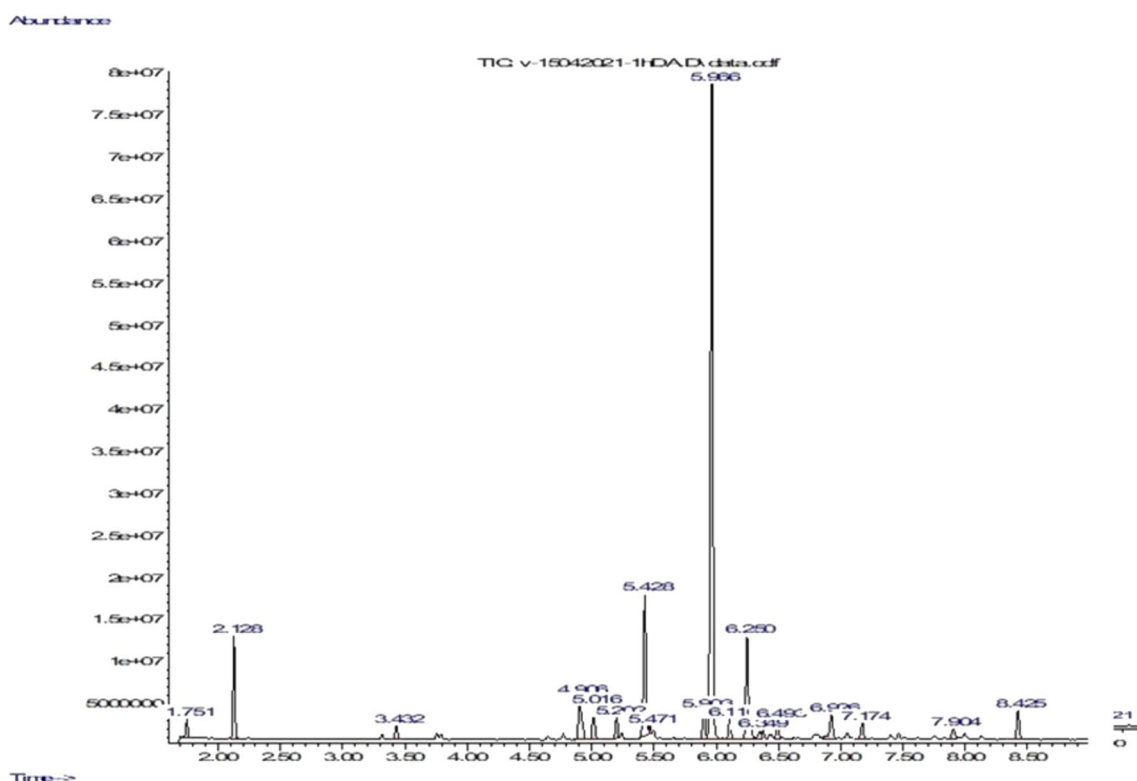


Fig. 1 Chromato-mass spectrum of pyrolysis oil

Table 3 Fractional composition of pyrolysis oil

Fractions, No	Temperature range, °C	Main product in the obtained fraction	Mass fraction of the product, %
1	179–189	Indene, 1-methylindene, tetralin	70.0
2	210–220	Naphthalene	96.0
3	220–235	Naphthalene, 1-methylnaphthalene, 2-methylnaphthalene	85.0
4	235–250	1-methylnaphthalene, 2-methylnaphthalene	88.0
5	250–260	Diphenyl	21.0
6	260–270	1,6-dimethylnaphthalene	40.1
7	270–280	Acenaphthene	50.0
8	280–290	Trimethyl naphthalene	75.0
9	290–300	Fullerene	52.0
10	–	The rest	

### Sulfonation of indene

The sulfonation of indene to produce indenesulfonic acid is a pivotal step in harnessing the chemical potential of indene for various industrial applications (Scheme 1). This process follows a methodology akin to the sulfonation of naphthalene series hydrocarbons, underscoring the adaptability of sulfonation techniques across different aromatic systems. Specifically, the reaction employs indene and sulfuric acid in a 1:1.2 molar ratio, maintained at a temperature range of

100–120 °C for four hours, culminating in a product yield of 71%. This efficient conversion rate highlights the practical viability of the process.

Following the reaction, the sulfo-mass undergoes a series of purification steps including mixing with water, treatment with  $\text{Ca}(\text{OH})_2$  solution for neutralization, and subsequent filtration to remove insoluble materials. Sodium carbonate is then added to the filtrate to precipitate the sodium salt of indenesulfonic acid, which is further purified through evaporation and drying. This multi-step purification ensures the

**Table 4** Chromato-mass spectrum results of fraction 1

No	Name	Mass percentage, %
1	Benzol	0.17
2	Ethylbenzene	0.29
3	Allylbenzene	0.30
4	1-Propylbenzol	0.48
5	1-Methyl-3-Ethylbenzol	6.16
6	1,2,4-Trimethylbenzol	4.00
7	1-Methyl-4-Ethylbenzol	3.25
8	C3-Benzol	28.92
9	Phenylethyl alcohol	0.50
10	1,2,3-Trimethylbenzol	4.53
11	1H- Indene	24.67
12	M-Propyltoluene	2.43
13	1,4-Dimethyl-2-Ethylbenzol	3.60
14	4-Ethyl-O-Xylene	1.77
15	1,3-Dimethyl-2-Ethylbenzol	2.60
16	1-Phenyl-2-Methylpropan	0.26
17	Bicyclohexane	0.44
18	5-Ethyl-m-Xylene	0.23
19	1-Methyl-2-Isopropylbenzol	1.93
20	O-Alkyltoluol	0.39
21	P-Methylallil Benzol	0.75
22	1-Methyl-Indene	2.85
23	1-Butinyl Benzol	1.47
24	Naphthalene	0.76
25	Azolin	5.62
26	Methylnaphthalene	0.22

removal of impurities and the achievement of a high-purity final product, evidenced by the formation of a yellowish-brown sodium salt of indenesulfonic acid.

The transformation of indene through sulfonation and the subsequent structural changes are meticulously confirmed through IR spectroscopy. Notably, the IR spectrum of indenesulfonic acid shows significant alterations when compared to indene, particularly in the disappearance of the OH group absorption at  $3427.66\text{ cm}^{-1}$ , which is a direct consequence of the sulfonation reaction. The introduction of the sulfo-group is further evidenced by the appearance of new absorption maxima at  $1095.42\text{ cm}^{-1}$ , characteristic of sulfo-groups, and the alteration in the absorption patterns associated with the aromatic ring, indicating the successful incorporation of the sulfonic acid group into the indene molecule.

Moreover, the comparison of IR spectra before and after sulfonation—indene (with peaks at  $3022, 2964, 1583, 1485, 1378, 785, 717, 691\text{ cm}^{-1}$ ) and indenesulfonic acid (with peaks at  $3449, 2960, 1179, 1018, 663\text{ cm}^{-1}$ )—reveals substantial changes in the molecular structure. These changes

include the shift and disappearance of certain peaks, signifying the alteration of chemical bonds and the formation of new functional groups as a result of the sulfonation process.

### Polycondensation of indenesulfonic acid

The analysis demonstrates that the sulfonation process incorporates a sulfo-group into the indene molecule, resulting in the formation of indenesulfonic acid (Scheme 2). This acid was subsequently subjected to a polycondensation reaction with 35% formalin inside a pressure vessel. For this reaction, formalin and indenesulfonic acid were combined in a 1:1.4 molar ratio, with the reaction conditions set at a temperature of  $100\text{--}110\text{ }^{\circ}\text{C}$  and a pressure of  $30\text{--}40\text{ atm}$ . The resultant solid, which is insoluble in water, underwent machining, washing, and was then heated at  $100\text{--}105\text{ }^{\circ}\text{C}$  for 12 h to ensure the completion of the polycondensation process. The final product, a cation exchange resin, was designated as the IESA cation exchanger.

### Study of chemical–physical properties of IESA cation exchanger

The study of the chemical–physical properties of the IESA cation exchanger reveals intriguing insights when compared with the commercial KU-2-8 cation exchanger. The analysis focuses on aspects such as moisture content, mass and volume ratios, static exchange capacity, and dynamic exchange capacity, providing a comprehensive understanding of the material's characteristics (Table 5). The IESA cation exchanger exhibited a moisture content of up to 29.4%, significantly lower than the KU-2-8's range of 48–58%. This lower moisture content suggests that the IESA cation exchanger may offer better performance in applications where minimal water retention is desirable. When comparing mass to volume ratio, the IESA cation exchanger has a comparative mass of  $695\text{ g/dm}^3$  with a volume of  $72\text{ dm}^3$  for 50 g of the exchanger. In contrast, KU-2-8 has a slightly higher density with a comparative mass of  $750\text{ g/dm}^3$  for a volume of  $67\text{ dm}^3$  for the same mass. This indicates that the IESA cation exchanger is less dense than KU-2-8, potentially affecting its efficiency and capacity in ion exchange processes. In terms of comparative volume, the IESA cation exchanger exhibits a slightly lower ratio ( $2.74\text{ sm}^3/\text{g}$ ) compared to KU-2-8 ( $2.8\text{ sm}^3/\text{g}$ ) for nearly identical masses. This minor difference suggests that both cation exchangers have similar porosity and surface area characteristics, which are critical for ion exchange efficiency. The total static exchange capacity shows that the IESA cation exchanger, despite a lower moisture content, has a comparable capacity ( $V_s$  values of 3.8, 11.4, and  $100\text{ cm}^3/\text{g}$ ) to KU-2-8 ( $V_s$  values of 2.8, 12.2, and  $100\text{ cm}^3/\text{g}$ ). This suggests that the IESA cation exchanger can hold a similar amount of ions for

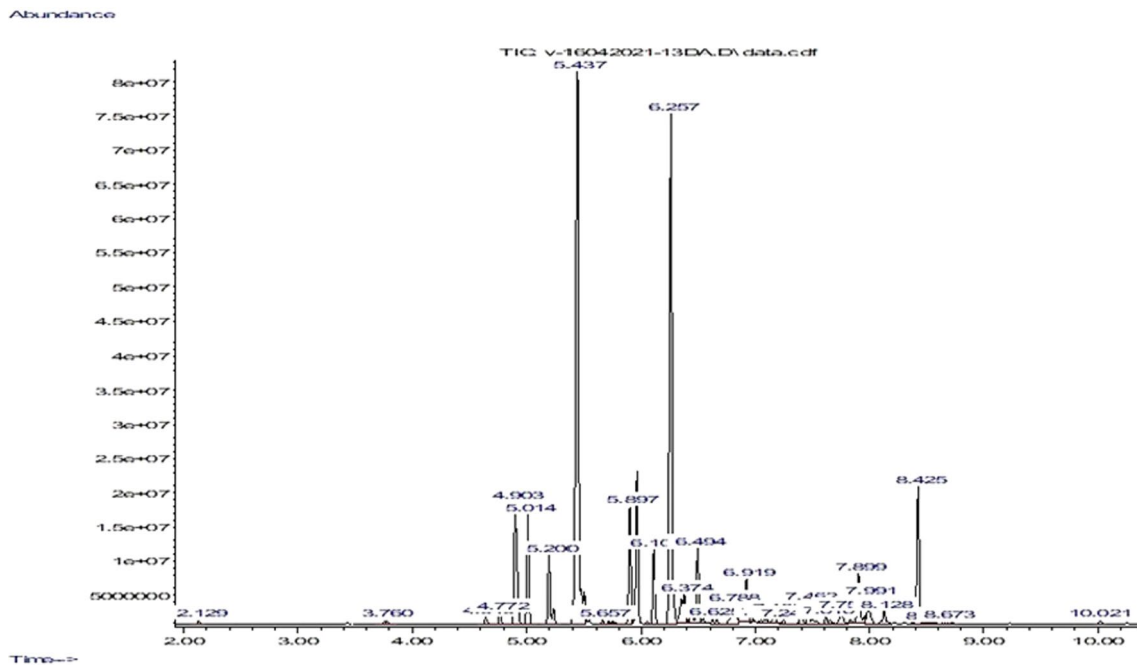
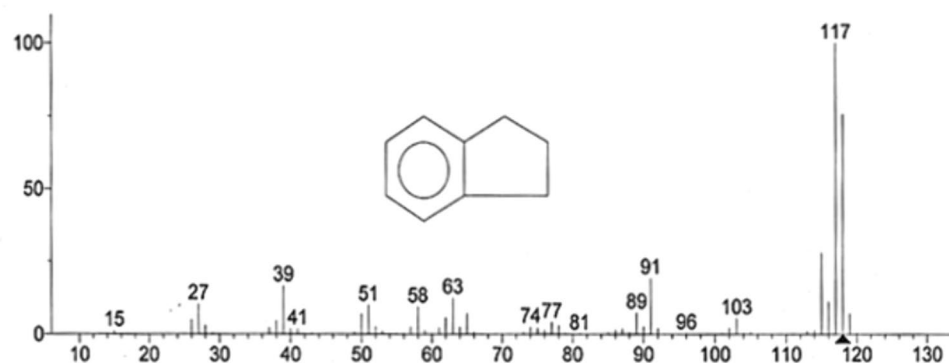


Fig. 2 Chromato-mass spectrum of fraction 1

Fig. 3 Chromo-mass spectrum of indene isolated from pyrolysis oil

Unknown: Indane  
Compound in Library Factor = 203



Hit 1 : Indane  
C9H10; MF: 999; RMF: 999; Prob 51.1%; CAS: 496-11-7; Lib: replib; ID: 16993.

exchange, which is impressive given its lower humidity. The dynamic exchange capacity (DEC) highlights a significant difference between the two cation exchangers. The IESA cation exchanger has a DEC of  $472 \text{ mmol/m}^3$ , which, while lower than KU-2-8's range of  $500\text{--}520 \text{ mmol/m}^3$ , suggests competitive performance. Furthermore, the volume increase from initial ( $V_i$ ) to final ( $V_f$ ) states shows that the IESA cation exchanger expands more (from  $100$  to  $258 \text{ m}^3$ ) than KU-2-8 (from  $100$  to  $292 \text{ m}^3$ ) under dynamic conditions, indicating a potentially higher resilience or flexibility during the ion exchange process (Fig. 5).

### IR analysis of IESA cation exchanger and its Na forms

The IESA cation exchanger displays a range of peaks at  $3365$ ,  $3067$ ,  $2955$ ,  $2926$ ,  $1603$ ,  $1449$ ,  $1151$ ,  $1027$ , and  $614 \text{ cm}^{-1}$ , with the broad peak at  $3365 \text{ cm}^{-1}$  indicating O–H stretching vibrations, suggesting hydroxyl groups or water presence (Fig. 6). Peaks at  $3067$  and  $2955 \text{ cm}^{-1}$  are associated with aromatic C–H and aliphatic C–H stretching, revealing a complex aromatic structure with alkyl substitutions. The  $2926 \text{ cm}^{-1}$  peak supports C–H stretching vibrations, and the absorption at  $1603 \text{ cm}^{-1}$  is likely



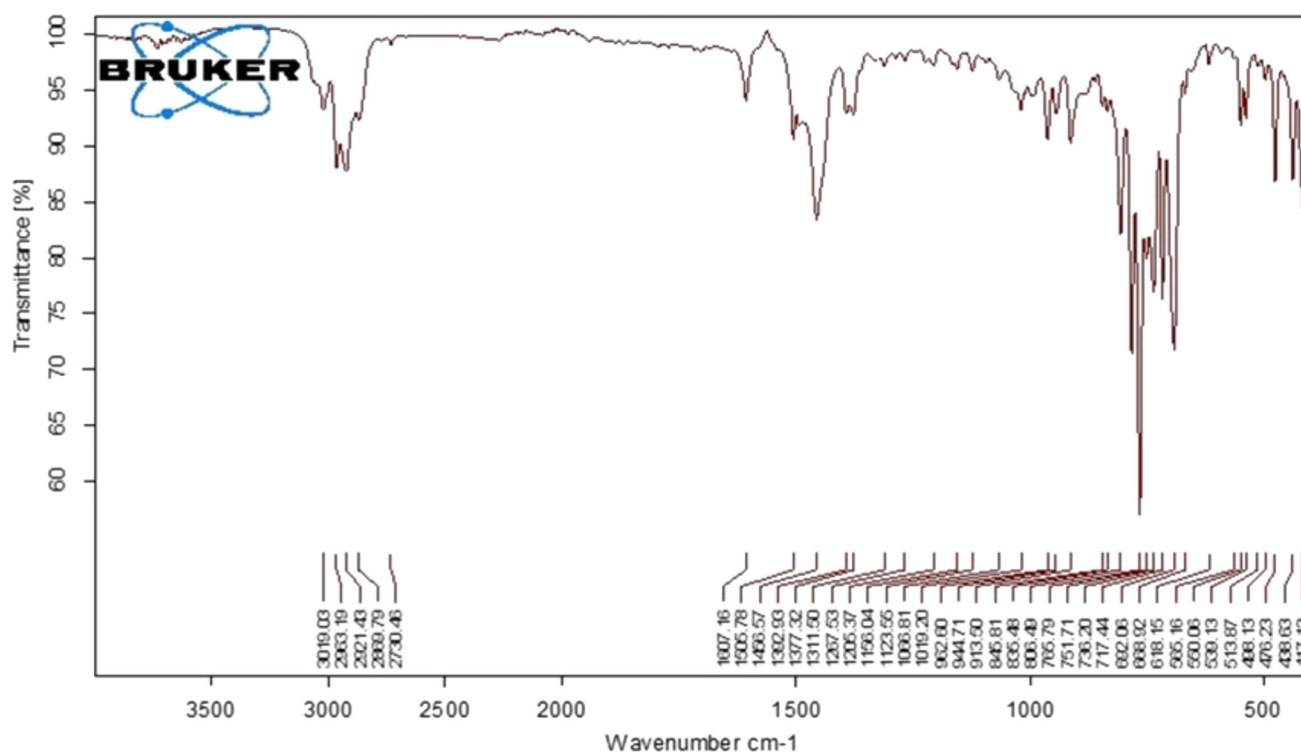
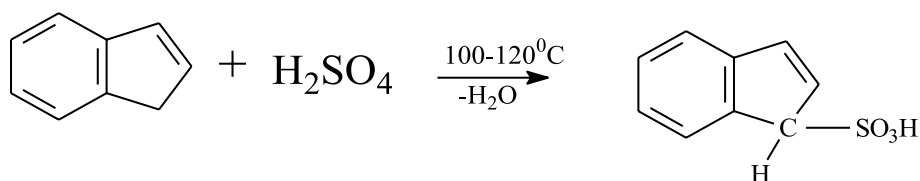


Fig. 4 IR spectrum of indene isolated from pyrolysis oil

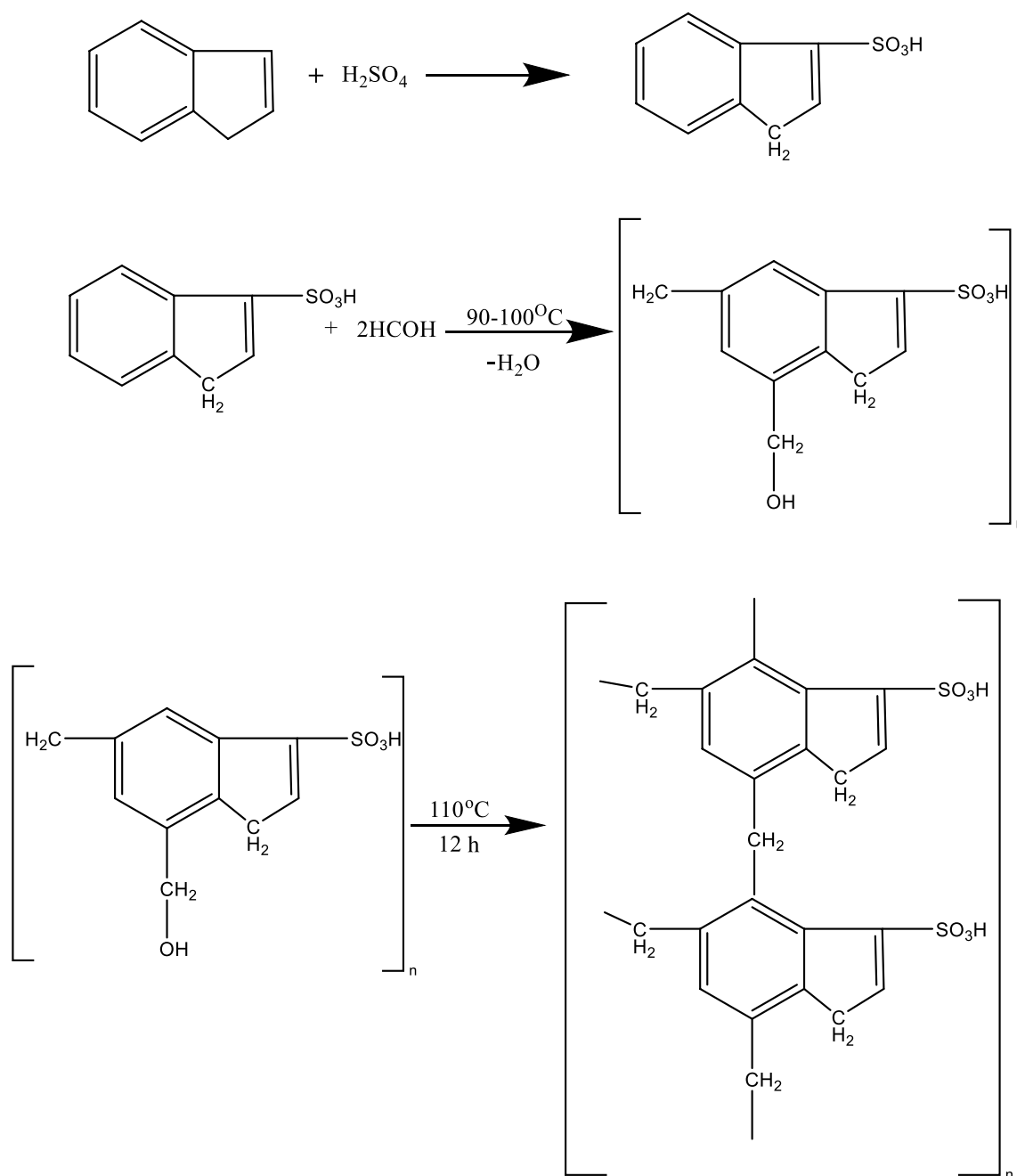
Scheme 1 Sulfonation reaction of indene



due to C=C stretching within aromatic rings, confirming the exchanger's aromatic nature. The 1449 and 1151  $\text{cm}^{-1}$  peaks are attributed to C-H bending and S=O stretching vibrations, indicating sulfonic acid groups, while the peak at 1027  $\text{cm}^{-1}$  signifies S-O stretching, and 614  $\text{cm}^{-1}$  may relate to out-of-plane C-H bending or metal-oxygen vibrations. The sodium salt form exhibits peaks at 3387, 2960, 1624, 1160, 1030, and 614  $\text{cm}^{-1}$ . The shift to 3387  $\text{cm}^{-1}$  from 3365  $\text{cm}^{-1}$  suggests changes in O-H stretching vibration due to sodium interaction. The peak at 2960  $\text{cm}^{-1}$ , slightly shifted from the exchanger form, aligns with aliphatic C-H stretching. A new peak at 1624  $\text{cm}^{-1}$  might indicate increased C=C stretching or changes in water binding to sodium ions. The 1160 and 1030  $\text{cm}^{-1}$  peaks suggest slight shifts in S=O and S-O stretching vibrations due to sodium presence, while the consistent peak at 614  $\text{cm}^{-1}$  in both forms points to unchanged structural features or functional groups post sodium exchange (Table 6).

### SEM and EDS analyses of IESA cation exchanger and its Na forms

The SEM image likely showcases the microstructural characteristics of the IESA cation exchanger, revealing its surface texture and porosity which are critical for ion exchange capabilities (Fig. 7). In Fig. 7a, the SEM image of the IESA cation exchanger reveals distinct changes including a porous surface texture essential for ion exchange capabilities, as the pores increase surface area for ion interaction. The image shows a granular structure with uniform distribution, indicating a consistent synthesis process and uniform ion exchange performance. While the SEM image itself does not display elemental composition, it is typically accompanied by EDS results highlighting the presence of key elements like carbon (C), oxygen (O), and sulfur (S), confirming the incorporation of sulfonic acid groups into the polymer matrix. The visible microstructural changes, such as the absence of significant cracks, suggest good mechanical integrity and stability of the



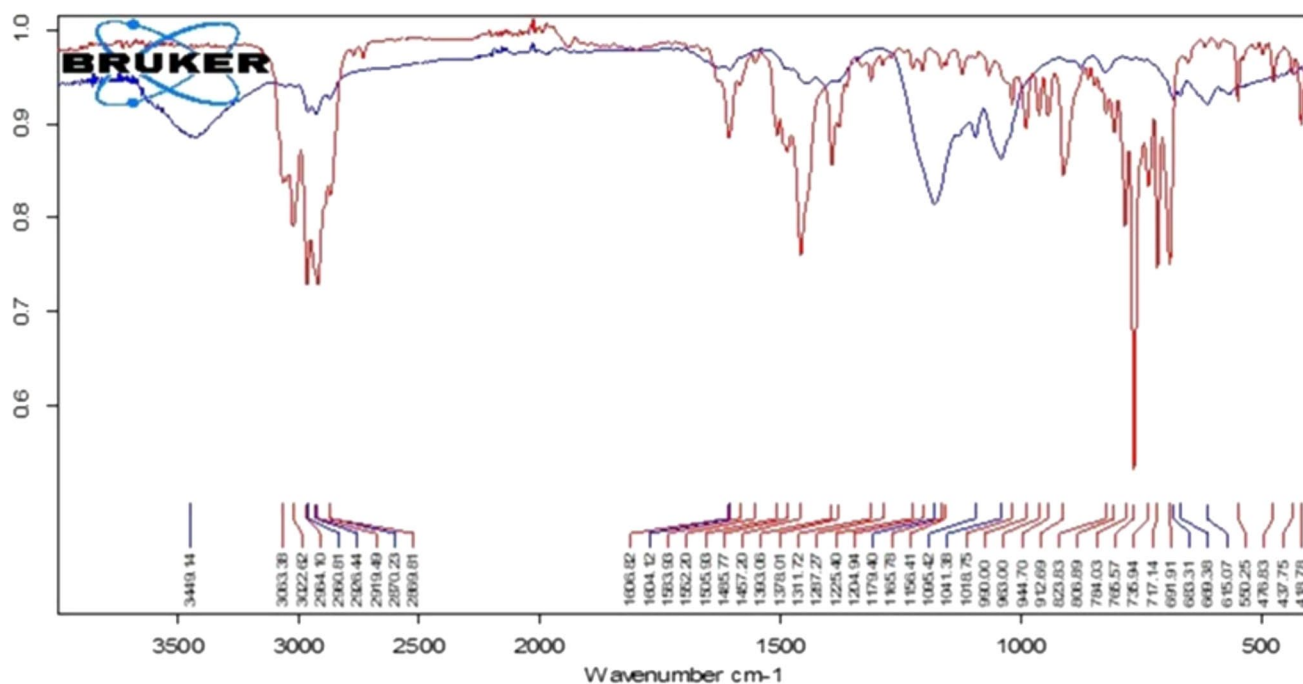
**Scheme 2** Reaction schema of synthesized cation exchanger based on indenesulfonic acid (IESA cation exchanger)

material, making the IESA cation exchanger suitable for practical ion exchange applications. The EDS results offer a quantitative breakdown of the elemental composition, highlighting a dominant carbon content (81.26% by mass), followed by oxygen (14.38%) and sulfur (4.36%). The high carbon percentage indicates the aromatic backbone of the polymer, essential for structural integrity and functionality. The presence of oxygen and sulfur at significant levels confirms the incorporation of sulfonic acid groups, pivotal for the cation exchange process.

The SEM images for the sodium forms of the IESA cation exchanger would similarly detail the microstructural changes upon sodium incorporation. These changes might include alterations in surface texture and porosity, affecting the material's ion exchange efficiency (Fig. 8). The EDS analysis shows a slight decrease in carbon content (77.70%) and sulfur (2.71%) with an increase in oxygen content (18.98%) compared to the non-sodium form. Notably, sodium appears in the composition at 0.60%, evidencing the successful exchange of hydrogen ions for sodium ions within the

**Table 5** Main chemical–physical properties of IESA cation exchanger and comparison with commercial KU-2–8

Comparative mass				
No	Cation exchangers	Mass (g)	Volume (dm <sup>3</sup> )	Comparative mass (g/dm <sup>3</sup> )
1	IESA cation exchanger	50	72	695
2	KU-2–8	50	67	750
Comparative volume				
No	Cation exchangers	Mass (g)	Volume (dm <sup>3</sup> )	Comparative volume (sm <sup>3</sup> /g)
1	IESA cation exchanger	15.004	29	2.74
2	KU-2–8	15.025	19	2.8
Total static exchange capacity				
No	Cation exchangers	Humidity, (%)	Mass (g)	V <sub>s</sub> (cm <sup>3</sup> /g), average V <sub>i</sub> (cm <sup>3</sup> ) and V <sub>f</sub> (cm <sup>3</sup> )
1	IESA cation exchanger	29.4	2.0001	3.8, 11.4 and 100
2	KU-2–8	58	2.085	2.8, 12.2 and 100
Dynamic exchange capacity				
No	Cation exchangers	Humidity, (%)	DOE (mmol/m <sup>3</sup> )	V <sub>i</sub> (sm <sup>3</sup> ), V <sub>f</sub> (sm <sup>3</sup> ) and average V <sub>n</sub> (sm <sup>3</sup> )
1	IESA cation exchanger	66	472	100, 150 and 258
2	KU-2–8	48–58	500–520	100, 172 and 292

**Fig. 5** IR spectrum of (red line) indene and (blue line) indenesulfonic acid

sulfonic acid groups. This exchange is crucial for the material's application in specific ion exchange scenarios, altering its selectivity and exchange capacity (Fig. 9).

Comparing the elemental composition of the IESA cation exchanger before and after sodium incorporation reveals

the successful modification of the material to its sodium form. The decrease in sulfur content and the appearance of sodium highlights the chemical changes that underpin the ion exchange capability of the material. Moreover, the increase in oxygen content in the sodium form suggests more

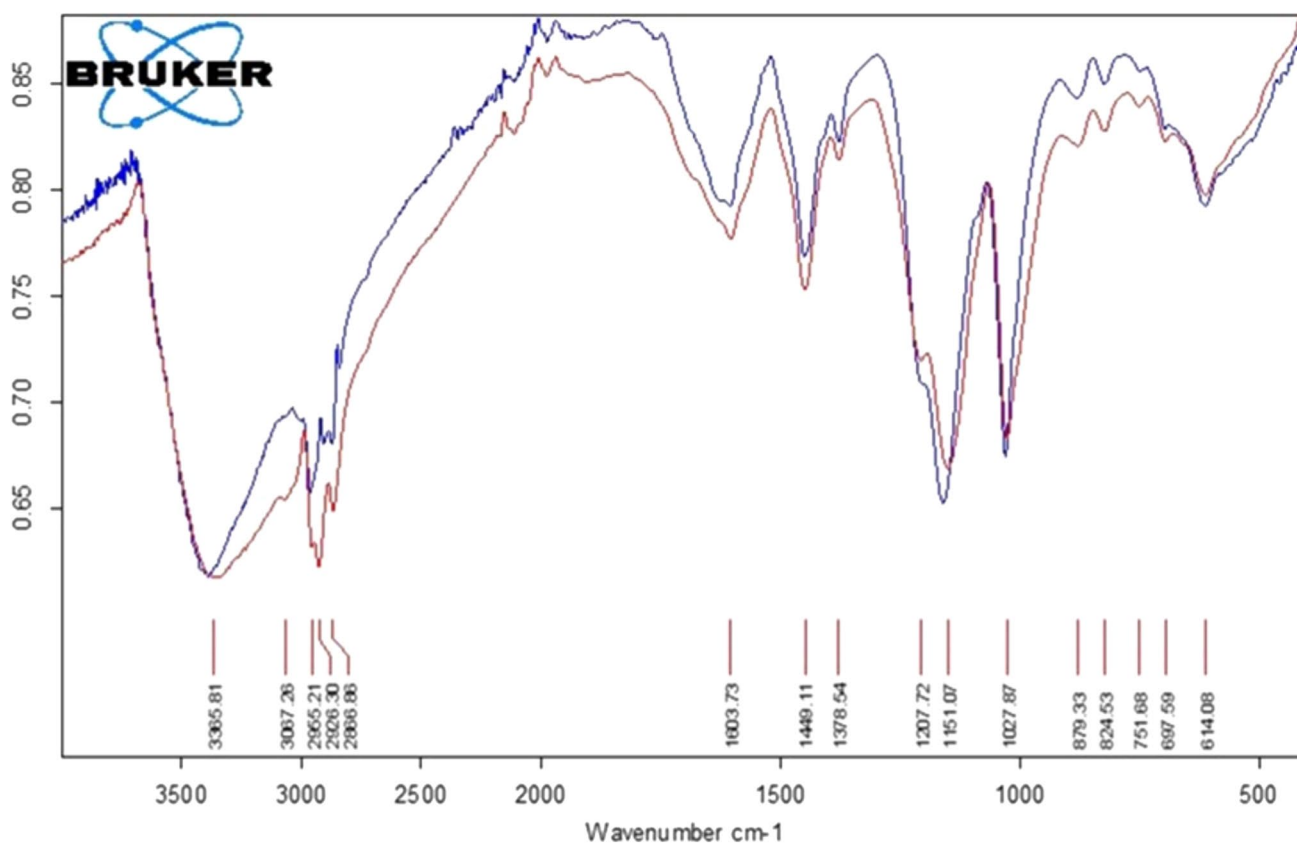


**Fig. 6** (Red line) IR analysis of IESA cation exchanger and (blue line) its sodium salt

pronounced ionic characteristics or changes in the sulfonic groups' environment due to sodium incorporation.

### TG analysis of IESA cation exchanger

The thermogravimetric (TG) analysis of the IESA cation exchanger provides a detailed view of its thermal stability and decomposition characteristics. The TG curves and accompanying data highlight the material's behavior under increasing temperatures up to 800 °C. Starting at room temperature (22 °C), the IESA cation exchanger shows negligible mass loss initially, with a slight decrease in mass signaled by a DTA value of  $-0.166 \mu\text{V}$ , indicating minimal evaporation or desorption of physically adsorbed water or solvents. As the temperature rises, a gradual increase in mass loss is observed, starting from 0.7734% at 30 °C, reaching 9.6783% by 100 °C, and continuing to rise steadily to 58.1727% at 800 °C. This pattern of mass loss reflects the material's thermal decomposition stages, including the loss of water, decomposition of organic constituents, and breakdown of sulfonic acid groups.

The rapidity of mass loss, calculated as mg/sec, varies throughout the heating process, with a notable increase in decomposition rate at higher temperatures. Initially, this

rate is relatively slow, indicating the thermal stability of the material at lower temperatures. However, as the temperature exceeds 100 °C, the rate of mass loss becomes more pronounced, with significant increases observed particularly beyond 250 °C. This suggests the onset of thermal decomposition of the polymer backbone and sulfonic groups. The differential thermal analysis (DTA) values, represented in microvolts ( $\mu\text{V}$ ), provide insights into the exothermic or endothermic nature of the decomposition reactions. Initially negative, the DTA values (in  $\mu\text{V}$ ) become positive as the temperature increases, peaking around 190 °C to 210 °C, indicating endothermic decomposition processes likely related to the loss of structural water or decomposition of sulfonic acid groups. Beyond 210 °C, the DTA values gradually decrease, suggesting a shift toward more exothermic decomposition reactions as the material breaks down further. Overall, the TG analysis of the IESA cation exchanger reveals its complex thermal behavior, with multiple stages of mass loss indicative of various decomposition processes. Understanding these thermal properties is crucial for optimizing the use of the IESA cation exchanger in real-world applications, ensuring its stability and functionality under the intended operating conditions.

**Table 6** TG results of IESA cation exchanger

No	Temperature, °C	Mass loss, %	Rapid of mass loss, mg/sec	DTA, $\mu$ V
1	22	–		–0.166000
2	30	0.7734	#DIV/0!	5.131001
3	40	2.0384	0.0008	8.334001
4	50	3.7276	0.0011	9.573000
5	60	5.4052	0.0012	10.523001
6	70	6.8665	0.0010	11.938000
7	80	7.9691	0.0008	13.419001
8	90	8.8891	0.0007	14.859001
9	100	9.6783	0.0006	15.939
10	110	10.2374	0.0004	16.778002
11	120	10.7153	0.0003	17.493000
12	130	11.1233	0.0003	18.008001
13	140	11.4568	0.0002	18.451000
14	150	11.8671	0.0003	18.651001
15	160	12.2367	0.0003	18.765001
16	170	12.6650	0.0003	19.014000
17	180	13.0482	0.0003	19.098000
18	190	13.3434	0.0002	19.227001
19	200	13.6883	0.0003	19.158001
20	210	14.0422	0.0003	18.916000
21	220	14.3756	0.0002	18.804001
22	230	14.7905	0.0003	18.536001
23	240	15.2480	0.0003	18.240000
24	250	15.8410	0.0004	17.743999
25	260	16.5602	0.0005	17.254002
26	270	17.3516	0.0006	16.903002
27	280	18.2084	0.0006	16.519001
28	290	19.0855	0.0006	16.354000
29	300	20.0506	0.0007	15.980001
30	310	21.0653	0.0007	15.584002
31	320	22.0371	0.0007	15.518002
32	330	23.0180	0.0007	15.753000
33	340	23.9853	0.0007	16.164001
34	350	24.9639	0.0007	16.839001
35	360	25.9334	0.0007	18.099001
36	370	26.8692	0.0007	19.212000
37	380	27.7620	0.0007	19.431000
38	390	28.6888	0.0003	19.182001
39	400	29.7554	0.0004	18.475000
40	410	30.9707	-0.0009	17.198000
41	420	32.2719	0.0009	16.297001
42	430	33.6587	0.0010	15.158001
43	440	35.1831	0.0011	13.833000
44	450	36.6917	0.0011	12.335001
45	460	38.2160	0.0011	10.608000
46	470	39.5510	0.0010	9.514000
47	480	40.7574	0.0009	8.068001
48	490	41.9164	0.0008	6.541000
49	500	43.0597	0.0008	4.938000

**Table 6** (continued)

No	Temperature, °C	Mass loss, %	Rapid of mass loss, mg/sec	DTA, $\mu$ V
50	510	44.2458	0.0008	3.374000
51	520	45.3033	0.0008	2.007000
52	530	46.3157	0.0007	0.434000
53	540	47.1454	0.0006	–0.931000
54	550	47.9685	0.0006	–2.659000
55	560	48.6989	0.0005	–3.864000
56	570	49.3912	0.0005	–5.218000
57	580	50.0743	0.0005	–6.530000
58	590	50.6062	0.0004	–7.476000
59	600	51.1744	0.0004	–9.077000
60	610	52.0357	0.0006	–10.236000
61	620	52.4933	0.0003	–11.224001
62	630	52.9374	0.0003	–12.433001
63	640	53.3161	0.0003	–13.616001
64	650	53.6767	0.0003	–14.676001
65	660	54.1006	0.0003	–15.803001
66	670	54.4340	0.0002	–16.688002
67	680	54.7609	0.0002	–17.670002
68	690	55.0133	0.0002	–18.432001
69	700	55.3333	0.0002	–19.727001
70	710	55.7052	0.0003	–20.551001
71	720	56.0343	0.0002	–21.300001
72	730	56.2980	0.0002	–22.413002
73	740	56.4939	0.0001	–23.145002
74	750	56.8320	0.0002	–24.278002
75	760	56.9671	0.0001	–25.142002
76	770	57.2487	0.0002	–26.067001
77	780	57.4898	0.0002	–27.002001
78	790	57.7896	0.0002	–27.874002
79	800	58.1727	0.0003	–28.773003

### Practical implications

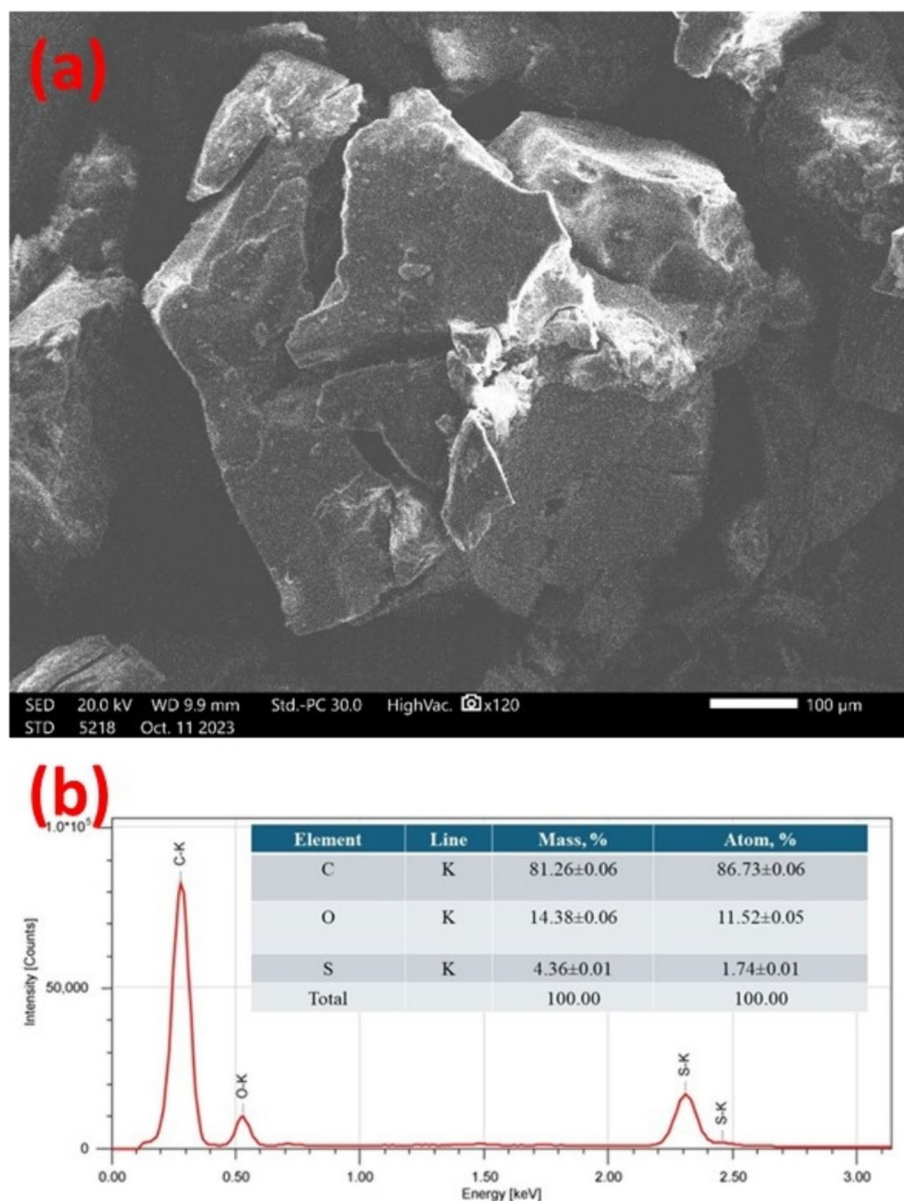
The findings from this study on the extraction of indene from pyrolysis oil and its subsequent conversion into a novel indene-based cationite (IESA cation exchanger) have several important practical implications:

*Sustainable Resource Utilization* The study demonstrates a viable method for transforming industrial by-products (pyrolysis oil) into high-value chemical products, promoting a circular economy and reducing waste. This approach can help industries minimize their environmental footprint and make better use of their resources.

*Enhanced Performance of Ion Exchange Resins* The synthesized IESA cation exchanger exhibits a significantly lower moisture content (29.4%) compared to commercial equivalents (48–58%). This characteristic is crucial for



**Fig. 7** **a** SEM and **b** EDS results of IESA cation exchanger



applications where minimal water retention is desirable, such as in water treatment and purification processes.

**Economic Benefits** By leveraging pyrolysis oil, a readily available industrial by-product, the process outlined in this study can lead to cost savings in the production of ion exchange resins. This makes the production process economically attractive, particularly for industries looking to reduce raw material costs.

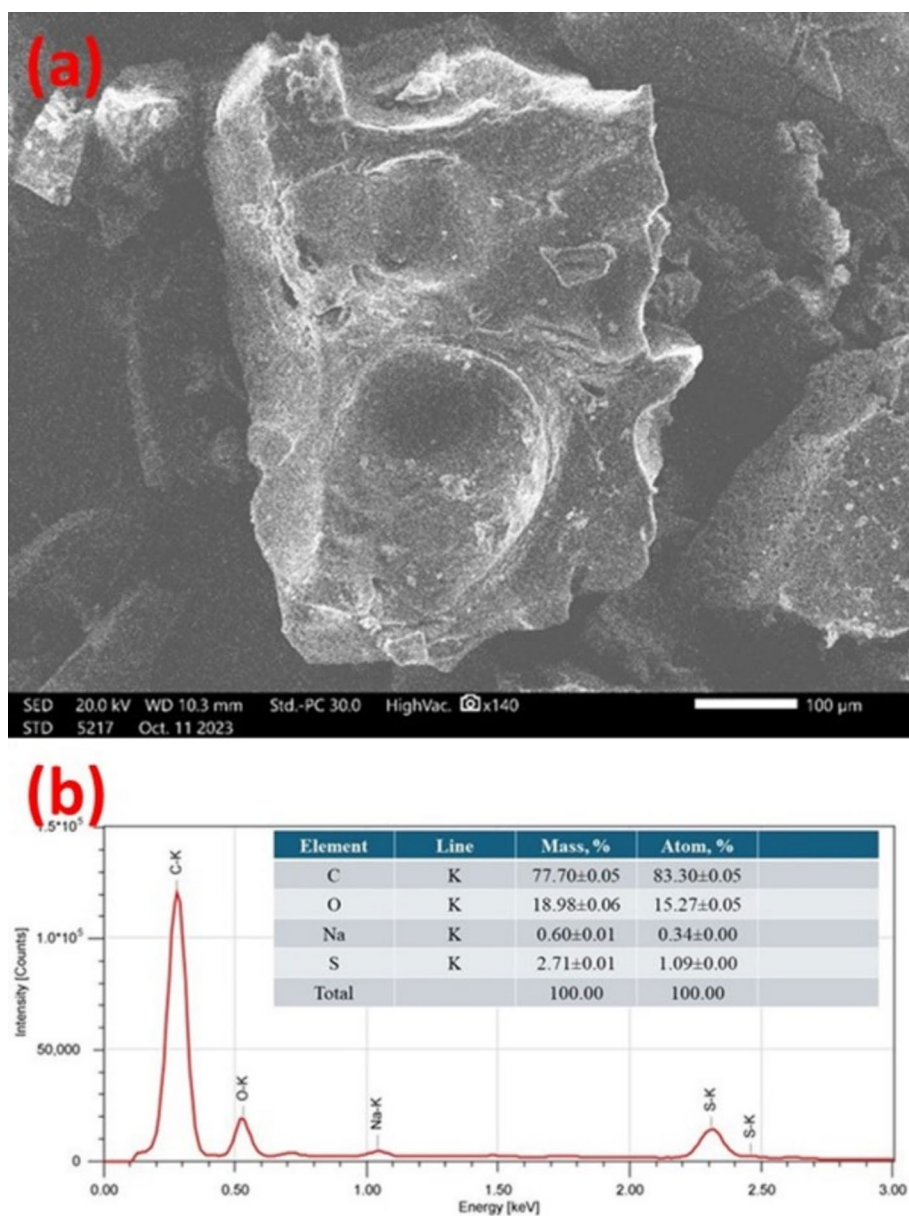
**Industrial Applications** The IESA cation exchanger's competitive dynamic exchange capacity (472 mmol/m<sup>3</sup>) compared to commercial standards (500–520 mmol/m<sup>3</sup>) suggests that it can be effectively used in various industrial applications, including water softening, wastewater treatment, and chemical processing.

**Environmental Impact** The research supports environmental sustainability by demonstrating the potential to utilize pyrolysis oil, which is otherwise considered waste, for the production of valuable chemicals. This contributes to reducing environmental pollution and supports the development of greener industrial processes.

**Thermal Stability and Durability** The thermal stability of the IESA cation exchanger up to 800 °C, as revealed by TG analysis, indicates its suitability for high-temperature applications. This makes it a robust material for environments requiring durable ion exchange resins.

**Innovative Material Development** The methodologies and processes developed in this study can be adapted to other aromatic hydrocarbons, potentially leading to the discovery and synthesis of new materials with unique

**Fig. 8** **a** SEM and **b** EDS results of IESA cation exchanger Na forms



properties. This innovation can drive advancements in material science and chemical engineering.

**Scalability and Commercialization:** The processes described for extracting indene and synthesizing the cationite are scalable, providing a pathway for commercial production. This facilitates the transition from laboratory research to industrial application, ensuring the practical utility of the findings.

By addressing these practical implications, the study not only advances scientific knowledge, but also provides actionable insights and solutions for industries looking to implement sustainable practices and improve their operational efficiency.

## Conclusion

The extraction of indene from pyrolysis oil and its transformation into a novel indene-based cationite (IESA cation exchanger) was successfully performed. The work yielded several key findings underscoring the potential of utilizing industrial by-products for sustainable chemical engineering applications. These findings represent significant advancements in knowledge and contribute to the fields of material science and chemical engineering:

*Efficient Indene Extraction* Utilizing advanced analytical techniques, indene was successfully isolated from pyrolysis oil, showcasing an efficient and effective extraction process.

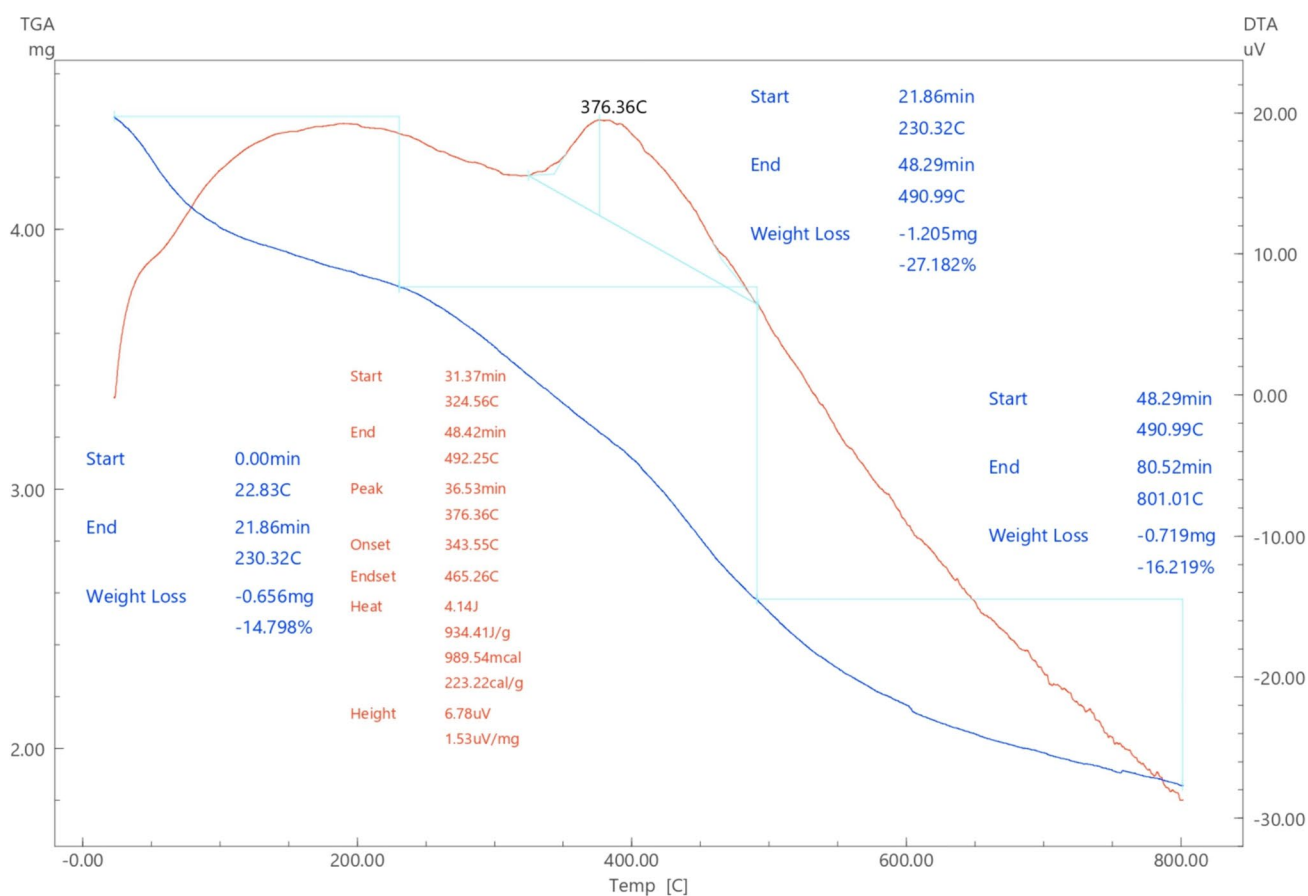


**Fig. 9** TG curves of IESA cation exchanger

**High Purity of Indene** Chromato-mass spectrometry revealed a principal ion peak at a molecular mass ( $m/z$ ) of 117.0, confirming the high purity of the extracted indene.

**Effective Sulfonation Process** The sulfonation of indene resulted in a product yield of 71%, indicating a highly effective reaction process.

**Improved Moisture Content** The synthesized IESA cation exchanger exhibited a moisture content of 29.4%, significantly lower than the commercial counterpart KU-2-8, which ranges from 48 to 58%. This lower moisture content suggests better performance in applications requiring minimal water retention.

**Density and Dynamic Exchange Capacity** The IESA cation exchanger demonstrated a comparative mass of  $695 \text{ g/dm}^3$  and a dynamic exchange capacity (DEC) of  $472 \text{ mmol/m}^3$ , showcasing competitive performance with commercial standards ( $500\text{--}520 \text{ mmol/m}^3$ ).

**Thermal Stability** TG analysis provided insights into the thermal behavior and stability of the IESA cation exchanger up to  $800^\circ\text{C}$ , highlighting its suitability for various applications.

**Elemental Composition** EDS analysis revealed the elemental composition of the IESA cation exchanger, including significant carbon content (81.26%) and the presence of sulfur (4.36%), essential for its functionality as a cation exchange resin.

**Sodium Incorporation** The sodium form of the IESA cation exchanger showed an elemental composition adjustment with sodium content at 0.60%, confirming successful ion exchange.

**Structural Insights** FT-IR analysis of the indene-based cation exchanger and its sodium salt form provided detailed insights into structural changes, with notable peaks indicating the presence and alteration of functional groups.

**Microstructural Characteristics** SEM analysis revealed the microstructural characteristics of the IESA cation exchanger and its sodium forms, important for understanding its ion exchange capabilities.

**Environmental Impact** This research highlights the sustainable potential of using pyrolysis oil as a feedstock for valuable chemical production, aligning with goals for environmental sustainability and efficient resource utilization.

These findings not only advance the understanding of pyrolysis oil valorization, but also demonstrate the practical feasibility of converting industrial by-products into high-value chemical products, promoting sustainable practices and efficient resource utilization in chemical engineering and material science.

## References


- Abusultan AAM et al (2024) A hybrid process combining ion exchange resin and bipolar membrane electrodialysis for reverse osmosis remineralization. *Desalination* 573:117209
- Al-Asheh S, Aidan A (2020) A comprehensive method of ion exchange resins regeneration and its optimization for water treatment. Promising techniques for wastewater treatment and water quality assessment 163–176
- Bakar MSA et al (2020) Pyrolysis of solid waste residues from Lemon Myrtle essential oils extraction for bio-oil production. *Biores Technol* 318:123913
- Busche SA et al (2024) Heavy metal on stage: making ion-exchange resin selective by peptide tetrazine-norbornene ligation. *Polymer* 291:126608
- Cai S et al (2023) Design, synthesis, and evaluation of PD-1/PD-L1 small-molecule inhibitors bearing a rigid indane scaffold. *Eur J Med Chem* 256:115468
- Choi J-W et al (2020) Sequential recovery of gold and copper from bioleached wastewater using ion exchange resins. *Environ Pollut* 266:115167
- Dixit F et al (2021) PFAS removal by ion exchange resins: a review. *Chemosphere* 272:129777
- Dong Z et al (2024) A comparative study of electrodeposition and sodium dithionite reduction for recovering gold in gold-rich solution from the adsorption of thiosulfate solution by ion exchange resin. *Sep Purif Technol* 328:125053
- Dumur F (2021) Recent advances on visible light photoinitiators of polymerization based on Indane-1, 3-dione and related derivatives. *Eur Polymer J* 143:110178
- Gong J et al (2024) Method for predicting lifetime of ion exchange resin in PWR primary loop based on nuclide distribution measurement. *Nucl Instrum Methods Phys Res, Sect A* 1059:168982
- Huang R et al (2021) Ion-exchange resins for efficient removal of colorants in bis (hydroxyethyl) terephthalate. *ACS Omega* 6(18):12351–12360
- Jasim AQ, Ajjam SK (2024) Removal of heavy metal ions from wastewater using ion exchange resin in a batch process with kinetic isotherm. *S Afr J Chem Eng* 49:43–54
- Ku C-E, Liu L, Zhang C (2024) Ion-exchange resin-templated carbon capture sorbents with hierarchical pores. *Ind Eng Chem Res* 63:11444–11452
- Kuan JY et al (2023) Organocatalytic vinylogous michael addition/cyclization cascade of 2-alkylidene indane-1, 3-diones with enals: a regio- and stereocontrolled diversity-oriented route to indane-1, 3-dione derivatives. *Adv Synth Catal* 365(20):3493–3504
- Lebron YAR, Moreira VR, Amaral MCS (2021) Metallic ions recovery from membrane separation processes concentrate: a special look onto ion exchange resins. *Chem Eng J* 425:131812
- Lee J-C et al (2020) Separation of platinum, palladium and rhodium from aqueous solutions using ion exchange resin: a review. *Sep Purif Technol* 246:116896
- Li X-R et al (2020) Controllable Tandem [3+ 2] Cyclization of Aromatic Aldehydes with Maleimides: Rhodium (III)-Catalyzed Divergent Synthesis of Indane-Fused Pyrrolidine-2, 5-dione. *Org Lett* 22(22):8808–8813
- Liao L, Zhao X (2022) Indane-based chiral aryl chalcogenide catalysts: development and applications in asymmetric electrophilic reactions. *Acc Chem Res* 55(17):2439–2453
- Mamchenko OV, Pakhar TA (2024) Combined technology of water softening, desalination, and deionization. *J Water Chem Technol* 46(2):125–131
- McCabe MN et al (2020) Off the beaten path: Almost clean formation of indene from the ortho-benzyne+ allyl reaction. *J Phys Chem Lett* 11(8):2859–2863
- Miettinen H et al (2024) The effects of indigenous microorganisms and water treatment with ion exchange resin on Cu-Ni flotation performance. *Miner Eng* 205:108473
- Munnangi SR et al (2024) Assessing Abuse-Deterrent formulations utilizing Ion-Exchange resin complexation processed via Twin-Screw granulation for improved safety and effectiveness. *Eur J Pharm Biopharm* 197:114230
- Oates CL et al (2023) Manganese catalysed enantioselective hydrogenation of in situ-synthesised imines: efficient asymmetric synthesis of amino-indane derivatives. *Green Chem* 25(10):3864–3868
- Pigot C, Brunel D, Dumur F (2022) Indane-1, 3-Dione: from synthetic strategies to applications. *Molecules* 27(18):5976
- Prisyazhnyi Y et al (2023) Resins with oxygen-containing functional groups obtained from products of fossil fuels processing: a review of achievements. *ChChT* 17:574–591
- Pyshyev S et al (2023) Bitumen Modified with Resins Obtained from Coal Coking Liquid Products: Nature, Adhesive and Rheological Properties
- Ramdas V et al (2020) Discovery of potent, selective, and state-dependent NaV1. 7 inhibitors with robust oral efficacy in pain models: structure-activity relationship and optimization of chroman and indane aryl sulfonamides. *J Med Chem* 63(11):6107–6133
- Rasouli Y et al (2024) Performance of biological ion exchange resin and gravity-driven ceramic membrane hybrid process for surface water treatment. *Sep Purif Technol* 332:125769
- Sarchami T, Batta N, Berruti F (2021) Production and separation of acetic acid from pyrolysis oil of lignocellulosic biomass: a review. *Biofuels, Bioprod Biorefin* 15(6):1912–1937
- Sekar M et al (2021) Combustion and emission characteristics of diesel engine fueled with nanocatalyst and pyrolysis oil produced from the solid plastic waste using screw reactor. *J Clean Prod* 318:128551
- Sekar M et al (2022) Production and utilization of pyrolysis oil from solidplastic wastes: a review on pyrolysis process and influence of reactors design. *J Environ Manage* 302:114046
- Sun K et al (2022) Sunlight induced polymerization photoinitiated by novel push-pull dyes: indane-1, 3-Dione, 1H-Cyclopenta [b] Naphthalene-1, 3 (2H)-Dione and 4-Dimethoxyphenyl-1-allylidene derivatives. *Macromol Chem Phys* 223(4):2100439
- Suo Y et al (2022) Ruthenium-Mediated [2+ 2+ 2] cyclization: a route to forge indane and isoindoline core and its application in dna-encoded library technology. *Org Lett* 24(49):9092–9096
- Tao J et al (2020) Multi-step separation of different chemical groups from the heavy fraction in biomass fast pyrolysis oil. *Fuel Process Technol* 202:106366
- Toteva V, Stanulov K (2020) Waste tires pyrolysis oil as a source of energy: Methods for refining. *Progress Rubber, Plast Recycl Technol* 36(2):143–158
- Vinco JH et al (2022) Purification of an iron contaminated vanadium solution through ion exchange resins. *Miner Eng* 176:107337
- Wang M et al (2024) New insight into polystyrene ion exchange resin for efficient cesium sequestration: the synergistic role of confined zirconium phosphate nanocrystalline. *Chin Chem Lett* 35(1):108442

- Yan Y et al (2024) Advanced treatment of wastewater by biological ion-exchange resin for dissolved organic carbon and pharmaceutical removal. *ACS ES&T Water* 4(4):1546–1555
- Zeidabadi FA et al (2024) Managing PFAS exhausted Ion-exchange resins through effective regeneration/electrochemical process. *Water Res* 255:121529
- Zhuang Z et al (2021) Rapid construction of tetralin, chromane, and indane motifs via cyclative C-H/C-H coupling: four-step total synthesis of (±)-russujaponol F. *J Am Chem Soc* 143(2):687–692

**Publisher's Note** Springer Nature remains neutral with regard to jurisdictional claims in published maps and institutional affiliations.

Springer Nature or its licensor (e.g. a society or other partner) holds exclusive rights to this article under a publishing agreement with the author(s) or other rightsholder(s); author self-archiving of the accepted manuscript version of this article is solely governed by the terms of such publishing agreement and applicable law.

## Authors and Affiliations

Saidmansur Saidobbozov<sup>1</sup> · Suvonqul Nurmanov<sup>1</sup> · Orifjon Qodirov<sup>1</sup> · Askar Parmanov<sup>1</sup> · Samadjon Nuraliyev<sup>1</sup> · Elyor Berdimurodov<sup>2,3,4</sup> · Ahmad Hosseini-Bandegharai<sup>5,6,7,8</sup>  · Wan Mohd Norsani B. Wan Nik<sup>9</sup> · Asmaa Benettayeb<sup>10,11</sup> · Nabisab Mujawar Mubarak<sup>12,13</sup> · Khasan Berdimuradov<sup>14,15</sup>

✉ Elyor Berdimurodov  
elyor170690@gmail.com

✉ Ahmad Hosseini-Bandegharai  
ahoseinib@semnan.ac.ir; ahoseinib@yahoo.com

<sup>1</sup> Department of General and Oil-Gas Chemistry, National University of Uzbekistan, Tashkent, Uzbekistan

<sup>2</sup> Chemical & Materials Engineering, New Uzbekistan University, 54 Mustaqillik Ave., 100007 Tashkent, Uzbekistan

<sup>3</sup> Department of Physical Chemistry, National University of Uzbekistan, 100034 Tashkent, Uzbekistan

<sup>4</sup> Physics and Chemistry, “Tashkent Institute of Irrigation and Agricultural Mechanization Engineers” National Research University, 100000 Tashkent, Uzbekistan

<sup>5</sup> Faculty of Chemistry, Semnan University, Semnan, Iran

<sup>6</sup> Department of Sustainable Engineering, Saveetha School of Engineering, SIMATS, Chennai, Tamil Nadu 602105, India

<sup>7</sup> Centre of Research Impact and Outcome, Chitkara University, Rajpura, Punjab 140417, India

<sup>8</sup> University Centre for Research & Development, Chandigarh University, Mohali, Punjab 140413, India

<sup>9</sup> Faculty of Ocean Engineering Technology and Informatics, Universiti Malaysia Terengganu, 21030 Kuala Nerus, Malaysia

<sup>10</sup> Laboratoire de Génie Chimique Et de Catalyse Hétérogène, Département de Génie Chimique, Université de Sciences Et de La Technologie -Mohamed Boudiaf, USTO-MB, BP 1505 EL-M'NAOUAR, 31000 Oran, Algeria

<sup>11</sup> Laboratoire Physico-Chimie des Matériaux – Catalyse et Environnement – LPCM-CE, Université des Sciences et de la Technologie d'Oran Mohamed Boudiaf (USTO-MB), BP 1505, El M'naouer, 31000 Oran, Algeria

<sup>12</sup> Petroleum and Chemical Engineering, Faculty of Engineering, Universiti Teknologi Brunei, Bandar Seri Begawan BE1410, Brunei

<sup>13</sup> Department of Chemistry, School of Chemical Engineering and Physical Sciences, Lovely Professional University, Jalandhar, Punjab, India

<sup>14</sup> University of Tashkent for Applied Sciences, Str. Gavhar 1, 100149 Tashkent, Uzbekistan

<sup>15</sup> Physics and chemistry, Western Caspian University, AZ-1001 Baku, Azerbaijan